Irradiation-enhanced adsorption and trapping of O_2 on nanoporous water ice

J. Shi, B. D. Teolis, and R. A. Baragiola*
Laboratory for Atomic and Surface Physics, Thornton Hall, University of Virginia, Charlottesville, Virginia 22904-4238, USA
(Received 17 February 2009; revised manuscript received 15 May 2009; published 18 June 2009)

We have found that irradiation with 50–150 keV protons enhances gas adsorption in nanoporous amorphous ice by creating high-energy binding sites. If irradiation is done in vacuum, the ice is compacted and does not adsorb significantly in subsequent exposure to gas. If irradiation occurs while the ice is exposed to an ambient O_2 pressure, adsorption is enhanced by a factor as high as 5.5 compared to unirradiated ice. The maximum concentration of adsorbed O_2 increased with increasing pressure and decreasing ion flux, achieving ~6% throughout the ion-penetration depth in the low-flux limit (at 7.2×10^{-5} mbar and 50 K). After simultaneous irradiation and oxygen exposure, the adsorbed O_2 could be retained in the ice when the ambient oxygen was removed, indicating that ion impacts close nanopores containing O_2. Similar results, but with somewhat lower gas/ice ratios where obtained with Ar, which has a lower binding energy than O_2. The experiments suggest a mechanism for gas trapping in comets and icy satellites in the outer Solar system.

DOI: 10.1103/PhysRevB.79.235422 PACS number(s): 34.35.+a, 68.43.Mn, 68.49.Sf

I. INTRODUCTION

When water vapor condenses from the gas phase onto a low-temperature (<100 K) substrate in vacuum, the deposited ice is amorphous and porous. Often called amorphous solid water (ASW), this material is ubiquitous in the outer solar system and in cold interstellar clouds. Among the peculiar properties of ASW is the internal network of nanoscale pores, which present a large effective surface area for gas absorption that can reach several hundred m^2/g.[1] The porosity is reduced irreversibly as amorphous ice is heated toward crystallization, which occurs at 130–160 K in time scales from hours to seconds. The many unusual properties of ASW,[2] including its extraordinary capacity for gas adsorption, continue to be expanded by research at several laboratories. Recent work has shown how growth conditions affect the porosity,[3,4] the type of pores,[5] and their destruction by ion irradiation.[6]

The gas-holding ability and long-exposure times have suggested that icy surfaces in the outer Solar system could be saturated with gases from their local environment. However, the very low gas density in the environment of those astronomical bodies means that even gases condensed with water will slowly desorb[7] except for a small fraction that stabilizes in structures, such as clathrates, upon crystallization.[7,8] Thus, retention of gases at low temperature in vacuum requires a mechanism that prevents desorption by, for instance, closing the pores containing gas. Pore collapse can result from heating, which also desorbs gas, or by irradiation with energetic particles typical of most astronomical environments.

This study sought to find if irradiation could help trap gases in ice and contribute to the understanding of observations of gases trapped on many objects in the outer solar system, including satellites of Jupiter and Saturn and ring particles. The choice of oxygen results from the fact that O_2 molecules are synthesized and ejected (sputtered) when the surface ice is irradiated by photons,[9] electrons,[10] and energetic ions from the solar wind and magnetospheric plasmas.[11,12] Sputtering is the main source of the tenuous O_2 atmospheres around Jupiter's satellites Europa and Ganymede,[13] and Saturn's rings.[14] Condensed O_2 was found on Jovian satellites[15] by the detection of weak absorption bands in the visible. The relationship between the condensed O_2-absorption feature and the tenuous O_2 atmospheres has long been a puzzle considering the instability of solid oxygen at the relative high temperatures of the satellites. Several aspects of the production and maintenance of these atmospheres have been modeled[16] assuming a negligible readsorption of atmospheric O_2 onto the icy surfaces of satellites and ring particles at their surface temperatures. In that context, we have re-examined the question of O_2 adsorption and retention in astrophysical ices, including the influence of ion irradiation. Here we report on our laboratory studies of the dependence of O_2 adsorption in ice films on temperature, pressure, thickness, and ion-irradiation history. A remarkable finding is that ion irradiation enhances adsorption of oxygen and its trapping in nanoporous water ice.

II. EXPERIMENTAL SETUP AND PROCEDURES

We conducted experiments in a cryopumped, stainless steel, ultrahigh vacuum chamber with a base pressure of 10^{-10} mbar. We prepared water-ice films by vapor deposition onto the surface of a liquid-helium-cooled gold-coated quartz-crystal microbalance using a collimating microcapillary array doser. To obtain a highly adsorbing microporous ice film we directed the collimated H_2O beam at an angle of 45° to the substrate surface.[3] Following preparation of the H_2O film, we leaked O_2 through the doser into the vacuum chamber to create background pressure and measured the mass uptake by the films using the microbalance, which has sensitivities of 0.07 and 0.04 ML for H_2O and O_2 (1 ML $=10^{15}$ molecules/cm^2). The doser was faced to the back of the cryostat during admission of O_2 to freeze out any remaining H_2O effusing from prior deposition of the ice film. A quadrupole mass spectrometer was used to measure the gas evolved during warming of the films, allowing an assessment of the purity of the H_2O and O_2 (>99.5%) and the composition of the desorbed flux. The background oxygen pressures were measured with a nude Bayard-Alpert gauge accu-

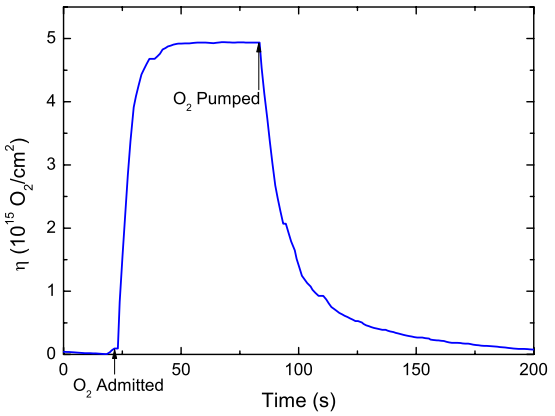

FIG. 1. (Color online) A typical adsorption and desorption curve at 60 K for a 5000 ML ice film grown at 60 K, exposed to an ambient O_2 pressure of 2×10^{-6} mbar.

rate to 20%. In some experiments ices were irradiated at normal incidence with a mass-analyzed collimated 100 keV Ar^+ or 50 keV H^+ beam from an ion accelerator. We also used infrared reflectance spectroscopy to look for the formation of absorbing species during irradiation. More details of the experimental setup can be found elsewhere.[17]

III. OXYGEN ADSORPTION WITHOUT IRRADIATION

Figure 1 shows the oxygen uptake increases asymptotically with time to a saturation value (O_2 pressure: 1.3×10^{-4} mbar) at which the O_2 adsorption and desorption rates are equal. When the sample chamber was pumped to ultrahigh vacuum, all O_2 desorbed from the film (within our sensitivity limit of 0.04 ML) and the time required for adsorbed O_2 to escape decreased with increasing temperature (e.g., 202, 27, and 4 s at 50, 60, and 65 K for 95% to escape), as expected from thermally activated desorption. Figure 2 shows the maximum column density η (O_2/cm^2) of oxygen adsorbed in two 60 K ice films of different thickness exposed

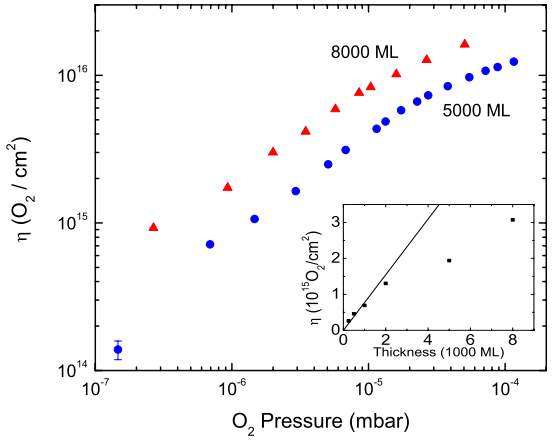

FIG. 2. (Color online) The column-density η of oxygen adsorbed by ice films 5000 and 8000 ML thick (1 ML $=10^{15}$ molecules/cm^2). The inset shows the O_2 uptake vs film thickness at an O_2 pressure of 7.2×10^{-7} mbar. Both the growth and absorption temperatures were 60 K.

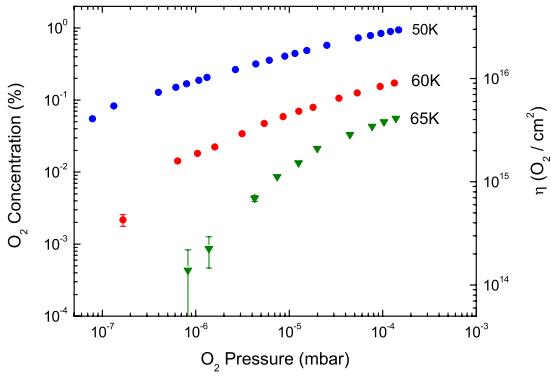

FIG. 3. (Color online) Concentration and column density of adsorbed oxygen vs pressure at different ice temperatures for 5000 ML thick ice films grown at 70 K.

to different O_2 pressures. The adsorption isotherm results from a dynamic competition between the transient adsorption due to an incoming O_2 flux (proportional to pressure) and thermal desorption. Additionally, the bottom-right inset in Fig. 2 shows that the oxygen uptake does not increase linearly with increasing film thickness, suggesting that nanopores deep in the film are less likely to be connected to the surface.

To investigate the effect of temperature on oxygen adsorption, we deposited ice films at 70 K and then exposed them to O_2 at different temperatures <70 K (we chose temperatures less than 70 K to avoid changes in porosity due to warming).[2] Figure 3 shows the resulting adsorption isotherms at 50, 60, and 65 K, where we chose to give oxygen concentrations obtained by dividing η by the column density of condensed water. The amount of O_2 dynamically adsorbed decreases with increasing ice temperature due to the increase in the O_2 desorption rate. The amount adsorbed at 80 K or above was below the sensitivity of the microbalance even at 10^{-4} mbar, which implies an adsorbed oxygen concentration $<0.0004\%$. Again, we found that all adsorbed O_2 left the film when oxygen was pumped from the chamber, which indicates that adsorbed O_2 is not trapped permanently in water ice at these temperatures. Figure 4 shows the saturation O_2 uptake vs temperature during exposure of a film deposited at 70 K to oxygen at 6.6×10^{-5} mbar. The porosity, ρ, of the film calculated from Fig. 4 shows $\rho\sim20\%$, assuming that adsorbed O_2 would not build up top layers prior to completely filling the micropores[5] and the fact the lowest temperature we measured, 31.5 K, is above the temperature (31.3 K) at which multilayer condensation begins at the pressure of 6.6×10^{-5} mbar. The temperature dependence is related to the distribution of adsorption-binding energies.[6]

IV. EFFECT OF ION IRRADIATION

Previous experiments have shown that ion irradiation reduces the porosity and gas-adsorption capacity of ASW in vacuum.[6] The next step was to study the simultaneous effect of exposing the ice to gas and irradiation since this is what occurs on satellite surfaces. As in our previous study using methane as the adsorbate,[5] we find here that irradiation be-

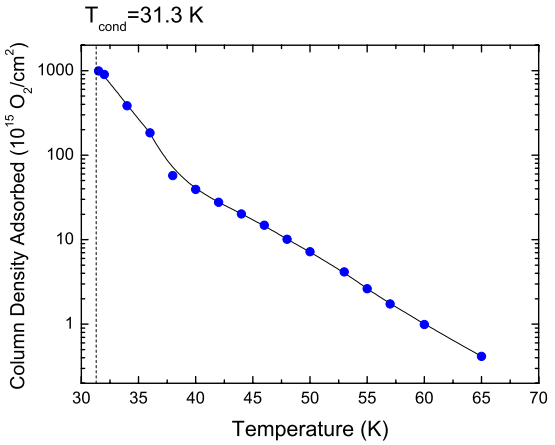

FIG. 4. (Color online) O_2 column density adsorbed on a 5000 ML ice film grown at 70 K and cooled to different temperatures, at a constant O_2 pressure of 6.6×10^{-7} mbar. At temperatures below 31.3 K (dashed line) multilayer condensation occurs at this pressure. The line following the data points is only to guide the eye.

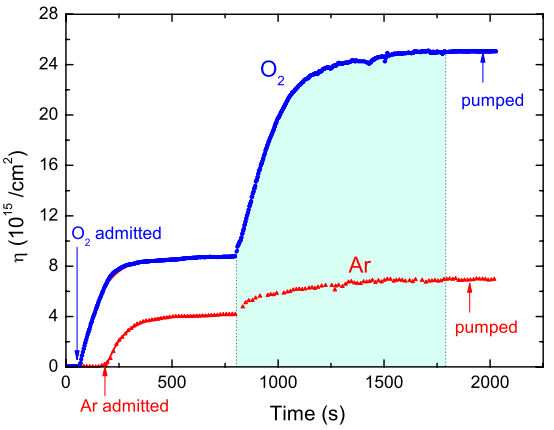

FIG. 5. (Color online) The O_2 and Ar column densities adsorbed at 50 K at a pressure of 7.2×10^{-7} mbar on a 5000 ML thick ice film grown at 70K. The shaded area indicates the period of irradiation with 50 KeV H^+ at a flux of $1.1(0.2)\times10^{12}$ ions cm^{-2} s^{-1} for O_2 (Ar). After the ambient gas was removed by pumping, no gas desorbed in the ice diffused out. The red line is a fit of the initial O_2 uptake using Eq. (4). We attribute the measured smaller Ar/ice ratio to lower binding energies to H_2O.

fore oxygen exposure reduces the O_2 adsorption, which we have demonstrated as follows: (i) we deposited a 5000 ML film at 70 K and cooled it to 50 K in vacuum. (ii) Then we irradiated the ice with 2×10^{15} Ar^+ ions cm^{-2}. (iii) After the irradiation, we exposed the film to 10^{-4} mbar O_2. Compared to the case without ion irradiation, which resulted in an adsorption of 4.3×10^{16} O_2/cm^2, the irradiated ice did not absorb O_2 above the detection limit of 4×10^{13} O_2/cm^2 (irradiation with 50 keV protons produced the same results). Since the penetration depth of the 100 KeV Ar^+ ions is much smaller than the total film thickness (about one sixth, or ~800 ML),[18] the results indicate that the altered surface layer prevents the penetration of O_2 molecules to the depths beyond the ion range, where the ice remains nanoporous. However, we point out that gases could still be adsorbed on the surface of heavily irradiated icy satellites since surface roughness, cracks, and other defects could allow shortcuts for gases to penetrate into depths unaffected by the magnetospheric ion irradiation.

Irradiation and oxygen adsorption are unlikely to be separated in time on a satellite surface; rather, they would take place simultaneously. However, in contrast to the case where irradiation is performed before oxygen exposure, irradiation enhances O_2 adsorption when carried out during exposure. This phenomenon is shown in Fig. 5, for a 5000 ML ice film deposited at 70 K, then exposed to an O_2 pressure of 7.2×10^{-7} mbar at 50 K. After attainment of saturation adsorption, we irradiated the ice with 50 KeV H^+ at a flux of 1.1×10^{12} ions/cm^2 s while maintaining the oxygen pressure. Additional O_2 adsorption began at the initiation of irradiation, increasing asymptotically to a new saturation level above a fluence of $\sim6\times10^{13}$ ions/cm^2 (Fig. 5). The additional adsorbed oxygen remained in the ice after irradiation and, remarkably, even after the oxygen exposure was stopped by removing the ambient O_2 gas.

On warming the ice, the adsorbed oxygen was retained in the film until the temperature rose above 140 K, indicating that the oxygen may escape during the sublimation of the water. Thus, in contrast to the case without irradiation, the binding of the adsorbed O_2 to the irradiated ice is sufficient to prevent its subsequent desorption. This increase in binding by irradiation suggests either (i) radiolytic dissociation of O_2 and water molecules followed by a recombination of radicals to form a species more strongly bound to the ice than O_2, or (ii) physical entrapment of adsorbed O_2 in pores collapsed by the irradiation. We can rule out a chemical explanation based on our infrared spectroscopy measurements, which show only the formation of 7.6×10^{15} molecules/cm^2 of H_2O_2 in the ice (above the saturation fluence of $\sim2\times10^{14}$ ions/cm^2). Since this amount is both similar to that produced by irradiation of ice in vacuum (i.e., no O_2 exposure)[19] and several times smaller than the total amount of trapped O_2, we conclude that the fraction of O_2 converted to H_2O_2 (or other species) is negligible. Moreover, enhanced adsorption is also observed for argon (Fig. 5): a phenomenon, which for this inert species cannot be attributed to radiation chemistry. Hence, the oxygen retention can only be attributed to trapping in collapsed nanopores; a conclusion supported by the similarity of the fluences required to saturate the enhanced adsorption (Fig. 6) and to collapse the pores.[6]

The irradiation-enhanced adsorption suggests a gradual process in which individual ions partially collapse a pore, thereby (i) entrapping the previously adsorbed O_2 while (ii) increasing the binding energy for adsorption of additional O_2 to previously unoccupied binding sites. An increase in binding energy would result, e.g., from a reduction in the pore width.[5] The competition between adsorption and pore collapse also produces a dependence of the adsorption on irradiation flux. This is shown in Figs. 6 and 7, where we have plotted O_2 adsorption vs fluence and its saturation value for different fluxes. The enhancement of adsorption is largest at the lowest fluxes, where the time between ion impacts is sufficient to allow maximum oxygen adsorption between pore-collapse events. In Fig. 7, we also note that at the larg-

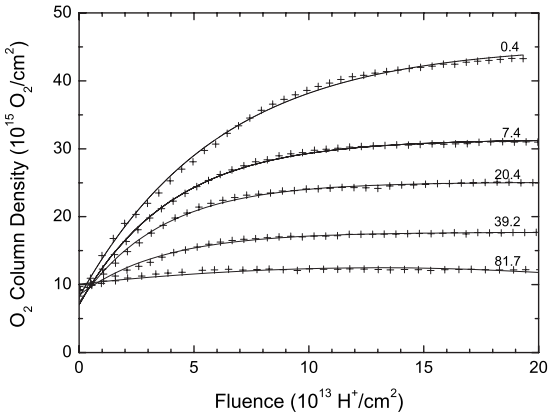

FIG. 6. The column density of O_2 adsorbed during 50 keV proton irradiation at 50 K of 5000 ML thick ice films grown at 70K at an ambient O_2 pressure of 7.2×10^{-7} mbar. The labels of each curve correspond to fluxes in units of 10^{10} ions cm^{-2} s^{-1}. Lines are fitted with Eq. (8).

est flux (2.2×10^{12} cm^{-2} s^{-1}); the total amount adsorbed is approximately equal to that obtained in the absence of irradiation, indicating the ion-induced enhancement at this flux almost disappears.

We also found that the irradiation-enhanced adsorption increases with film thickness, as shown in Figs. 8 and 9 for a flux of 2×10^{11} ions/cm^2/s. The linear growth of the enhancement with thickness and subsequent saturation above ~2000 ML is in reasonable agreement with the thickness dependence of the deposited energy, calculated with the Monte Carlo code TRIM,[18] as shown in Fig. 9. Considering the thickness dependence of the irradiation enhancement, we expect an oxygen molecular concentration of ~3% throughout the top 1000 ML at an ambient O_2 pressure of 7.2×10^{-7} mbar, in the limit of low fluxes. At an ambient pressure of 7.2×10^{-5} mbar, the enhanced concentration increases to ~6% in the same depth.

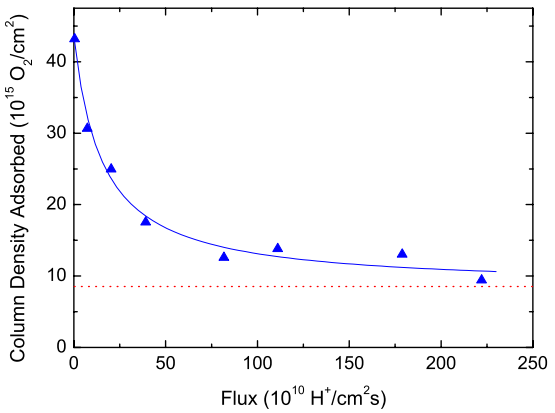

FIG. 7. (Color online) The total column density of O_2 trapped at 50 K in 5000 ML thick ice films grown at 70K vs the flux of 50 keV protons, with an O_2 pressure of 7.2×10^{-7} mbar using a total fluence of 2×10^{14} ions/cm^2. After each experiment, the trapped O_2 remained in the ice after the O_2 pressure was removed. The triangles are the experimental data and the line is a fit with Eq. (9). The dashed horizontal line is the average value of the saturation oxygen uptake in the absence of irradiation.

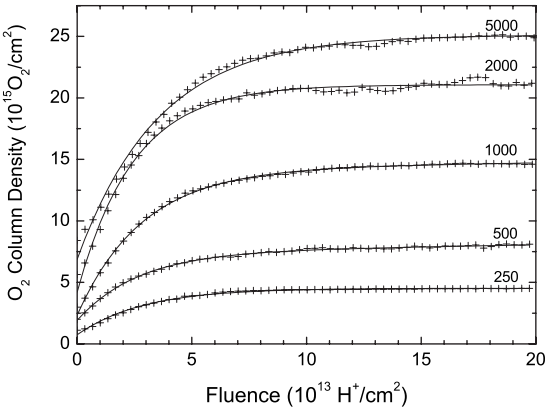

FIG. 8. Fluence dependence of the total O_2 trapped at 50 K for films of different thickness (in units of 10^{15} H_2O/cm^2) irradiated with a flux of $2\times10^{11}/cm^2$ s 50 keV protons. The crosses are the experimental data and the lines are fits to Eq. (8).

V. DISCUSSION

We first consider the adsorption kinetics in the absence of irradiation, where the rate of change of N, the amount of gas adsorbed, is given by the difference between the adsorption and desorption rates

$$N' = rP - DN. \tag{1}$$

Here, the prime denotes the derivative with respect to time t, P is the gas pressure, $r=s\beta\kappa$ is the adsorption coefficient, D is the desorption coefficient, s is the sticking probability, β the fraction of the surface open to the pores, and κ the constant, given by gas kinetic theory, that relates pressure to the flux of the incoming molecules. The ice films are heterogeneous, with a distribution of sites i with different binding energies ε_i for gas adsorption, as shown in previous studies on methane,[5] deuterium,[20] and nitrogen adsorption.[21] The coefficients s_i and D_i, are functions of ε_i and T. In our study with methane we analyzed the equilibrium isotherms with the condensation approximation,[22] which treats the strong dependence of D on binding-energy ε as an infinite step,

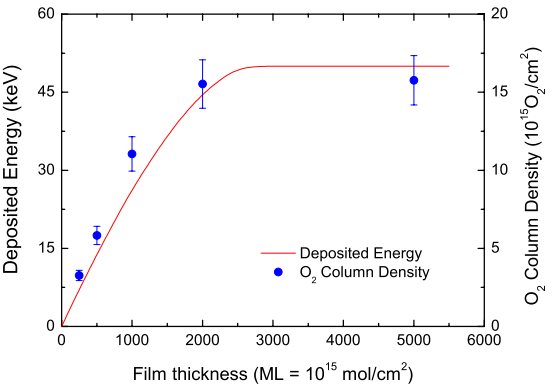

FIG. 9. (Color online) The column density of adsorbed O_2 enhanced by irradiation vs film thickness. The films were grown at 70 K and the irradiations were done at 50 K. The line is the energy deposited by 50 keV protons up to a given thickness, calculated using TRIM.

where $D=0$ for sites with binding energy above a value $\varepsilon_0(P,T)$, and infinity for sites with $\varepsilon<\varepsilon_0(P,T)$. The adsorbed molecules migrate rapidly by surface diffusion[5,23] and stick to the strongest available binding sites, and one can define N_M, a maximum value of N below which nearly all the occupied sites have binding energies higher than $\varepsilon_0(P,T)$ (hence $D=0$). Therefore, the desorption term can be dropped from Eq. (1) for $N<N_M$,

$$N' \approx rP \quad \text{for} \quad N < N_M. \tag{2}$$

In other words, N_M is the saturation value of N since for $N>N_M$, the molecules adsorbed at sites with $\varepsilon_i<\varepsilon_0(P,T)$ rapidly desorb. The experiments (Fig. 5) indeed show an initial linear dependence of uptake on time,

$$N = rPt, \tag{3}$$

where r is a constant. The initial slope of the uptake (Fig. 5) is $N' \approx 7\times10^{13}$ O_2 cm^{-2} s^{-1}. The incident flux is $\kappa P, = 7.2\times10^{-7}$, and therefore the fraction of the surface open to pores is $\beta = N'/s\kappa P = 0.35$ within 20%, the uncertainty in the pressure. To obtain this value, we have assumed $s=1$ since at low uptake most binding sites with $\varepsilon>\varepsilon_0(P,T)$ are unoccupied and available for adsorption. A somewhat lower value of β would result if one considers the small probability that molecules landing between pore openings diffuse on the surface and then enter the pore network. If the pores are distributed in an isotropic network, the value of β gives a bulk porosity of $\beta^{3/2} \approx 0.21$, is consistent with the porosity ($\sim$20%) calculated from Fig. 4 (see above), and in agreement with expectations based on previous measurements.[5]

The gas uptake slows down near N_M. Here the observed time evolution is better described by the assumption that the sticking probability is proportional to the number of unoccupied sites: $s \propto N_M - N$,

$$N' = a(N_M - N)P = aPN_H \therefore N = N_M[1 - \exp(-aPt)], \tag{4}$$

where $N_H = N_M - N$ is the number of unoccupied binding sites $[\varepsilon>\varepsilon_0(P,T)]$, and a is a constant. The fit of Eq. (4) to the data (Fig. 5) yields $a = 1.70\pm0.03\times10^4$ s^{-1} mbar^{-1}.

The inclusion of irradiation into the model requires that we consider two additional effects: (i) the increase in binding energy of an empty adsorption site from a state with ε below $\varepsilon_0(P,T)$ to above, making it available for adsorption, and (ii) complete pore collapse, which destroys empty available sites. These effects are described by the following coupled differential equations:

$$N' = aPN_H, \tag{5}$$

$$N_H' = \sigma JN_L - \gamma JN_H - aPN_H, \tag{6}$$

$$N_L' = -\sigma JN_L, \tag{7}$$

where N_L and N_H are the number of empty sites with binding energy below and above $\varepsilon_0(P,T)$, respectively, J is the ion flux, σ is the cross section for converting empty sites from low $[\varepsilon<\varepsilon_0(P,T)]$ to high $[\varepsilon>\varepsilon_0(P,T)]$ binding energies, and γ is the cross section for complete pore collapse. We note that N contains components from both transiently adsorbed O_2 (i.e., oxygen that desorbs upon removal of the ambient gas) and oxygen permanently enclosed in collapsed pores. We did not include in Eqs. (5)–(7) O_2 desorption by irradiation (sputtering) since molecules in only a shallow region of the ice can be removed from their binding sites and not re-adsorb on their way to the surface. We also did not consider ozone formation based on two arguments: (i) similar results were obtained with argon gas (Fig. 5), which show a lower uptake than oxygen, expected due to a lower binding energy and (ii) the maximum O_3:O_2 ratio in ion-irradiated O_2 water mixtures is $\ll 1$.[24]

Solving Eq. (5)–(7) for $N(t)$ yields

$$N(t) = N(0) + N_L(0) \times \frac{aP}{aP+\gamma J-\sigma J}\left\{1 - e^{-\sigma Jt} - \frac{\sigma J}{aP+\gamma J}[1 - e^{-(aP+\gamma J)t}]\right\}, \tag{8}$$

where $N(0)$ is the amount of O_2 adsorbed at the start of the irradiation, and we have assumed $N_H(0)=0$ since we obtained equilibrium adsorption prior to irradiation (i.e., all available adsorption sites were occupied). Within this model, pore collapse by irradiation explains why the adsorbed gas molecules remain trapped after the ambient gas was pumped out.

A. High fluence behavior

By taking $t\to\infty$ in Eq. (8), we obtain an expression for the flux dependence of saturation O_2 adsorption,

$$N_{\text{sat}}(J) = N(0) + \frac{aP}{aP+\gamma J}N_L(0). \tag{9}$$

The fit of Eq. (9) to the data of Fig. 7 yields good agreement for $N_L(0) = 3.5\pm0.2\times10^{16}$ cm^{-2} and $\gamma = 8\pm1\times10^{-14}$ cm^2. Using these results to constrain the fit of Eq. (8) to the time-dependent measurements of N (see Fig. 6), we obtain $\sigma = 3.3\pm0.1\times10^{-14}$ cm^{-2}. We note that $N_{\text{sat}}(0)$ at 50 K is five times larger than in the absence of irradiation and 5% of the maximum gas that can be accommodated in the pores at low temperatures (Fig. 4). The 5% value is explained by the fact that a lower amount of gas is found at the pores when an ion penetrates, due to the higher probability of desorption at 50 K.

B. Low flux behavior

In the limit of low fluxes ($J \ll aP/\gamma$), typical of astronomical environments, Eq. (8) reduces to

$$N(t\to0) = N(0) + \frac{1}{2}aP\sigma N_L(0)Jt^2,$$

$$N(t\to\infty) = N(0) + N_L(0). \tag{10}$$

Thus, at long times, $\gg 1/(aP)$, the gas fills all the adsorption sites present in the material, irrespective of their initial binding energy, which can be filled within the constraints of temperature and pressure.

VI. CONCLUSIONS

The experiments have unveiled a physical phenomenon, in which gas adsorption in nanoporous amorphous ice is enhanced by irradiation, due to the increase in binding energy at sites inside the micropores. In addition, irradiation closes pores containing oxygen leading to trapping. We observed similar results using Ar gas instead of oxygen. Enclosure in the pores is sufficiently effective that the adsorbed gas is permanently trapped in the ice, until desorption of the ice above 140 K. Irradiation of the ice prior to exposure to the gas reduces adsorption due to pore collapse.

The finding that ion-enhanced absorption is maximum in the limit of low fluences is important for astronomical applications. The synergistic effect between oxygen exposure and ion irradiation discussed here will also occur with other atmospheric constituents, not just oxygen, and result in surfaces containing a sample of atmospheric gases. Significant enhancements in gas adsorption and trapping should also be induced by energetic electrons and, possibly, by far UV photons, such as Lyman-α, since these types of irradiation are known to alter the structure of ice.[2] A detailed comparison of different processes and applications to astronomy are outside the scope of this work and will be published separately.

Finally, the results may be transferable to other types of nanoporous solids, such as zeolites, with potential application to gas storage.

ACKNOWLEDGMENTS

This research was supported by the NASA Planetary Atmospheres and Cassini programs through the Southwest Research Institute and JPL and by NSF Astronomy.

*Corresponding author; raul@virginia.edu

[1] E. Mayer and R. Pletzer, Nature (London) **319**, 298 (1986).
[2] R. A. Baragiola, Planet. Space Sci. **51**, 953 (2003).
[3] M. S. Westley, G. A. Baratta, and R. A. Baragiola, J. Chem. Phys. **108**, 3321 (1998).
[4] K. P. Stevenson, G. A. Kimmel, Z. Dohnalek, R. S. Smith, and B. D. Kay, Science **283**, 1505 (1999).
[5] U. Raut, M. Famá, B. D. Teolis, and R. A. Baragiola, J. Chem. Phys. **127**, 204713 (2007).
[6] U. Raut, B. D. Teolis, M. J. Loeffler, R. A. Vidal, M. Famá, and R. A. Baragiola, J. Chem. Phys. **126**, 244511 (2007); M. E. Palumbo, Astron. Astrophys. **453**, 903 (2006); U. Raut, M. Famá, M. J. Loeffler, and R. A. Baragiola, Astrophys. J. **687**, 1070 (2008).
[7] R. A. Vidal, D. Bahr, R. A. Baragiola, and M. Peters, Science **276**, 1839 (1997); R. A. Baragiola and D. A. Bahr, J. Geophys. Res. **103**, 25865 (1998).
[8] A. Bar-Nun, G. Herman, D. Laufer, and M. L. Rappaport, Icarus **63**, 317 (1985); A. Bar-Nun, J. Dror, E. Kochavi, and D. Laufer, Phys. Rev. B **35**, 2427 (1987).
[9] M. S. Westley, R. A. Baragiola, R. E. Johnson, and G. Baratta, Nature (London) **373**, 405 (1995); Planet. Space Sci. **43**, 1311 (1995).
[10] M. T. Sieger, W. C. Simpson, and T. M. Orlando, Nature (London) **394**, 554 (1998); N. G. Petrik, A. G. Kavetsky, and G. A. Kimmel, J. Phys. Chem. B **110**, 2723 (2006).
[11] W. L. Brown *et al.*, Nucl. Instrum. Methods Phys. Res. **198**, 1 (1982).
[12] B. D. Teolis, R. A. Vidal, J. Shi, and R. A. Baragiola, Phys. Rev. B **72**, 245422 (2005).
[13] R. E. Johnson, L. J. Lanzerotti, W. L. Brown, and T. P. Armstrong, Science **212**, 1027 (1981); D. T. Hall, D. F. Strobel, P. D. Feldman, M. A. McGrath, and H. A. Weaver, Nature (London) **373**, 677 (1995); M. Shi, R. A. Baragiola, D. E. Grosjean, R. E. Johnson, S. Jurac, and J. Schou, J. Geophys. Res. **100**, 26,387 (1995).
[14] R. L. Tokar *et al.*, Geophys. Res. Lett. **32**, L14S04 (2005); R. E. Johnson *et al.*, Icarus **180**, 393 (2006).
[15] J. R. Spencer, W. M. Calvin, and M. J. Person, J. Geophys. Res. **100**, 19049 (1995); J. R. Spencer and W. M. Calvin, Astron. J. **124**, 3400 (2002).
[16] V. I. Shematovich, R. E. Johnson, J. F. Cooper, and M. C. Wong, Icarus **173**, 480 (2005); J. Saur and D. F. Strobel, Astrophys. J. **620**, L115 (2005); W. H. Smyth and M. L. Marconi, Icarus **181**, 510 (2006).
[17] R. A. Vidal, B. D. Teolis, and R. A. Baragiola, Surf. Sci. **588**, 1 (2005).
[18] J. F. Ziegler and J. P. Biersack, TRIM 2006 (srim.org.).
[19] M. J. Loeffler, B. D. Teolis, and R. A. Baragiola, Astrophys. J. **639**, L103 (2006).
[20] L. Amiaud, J. H. Fillion, S. Baouche, F. Dulieu, A. Momeni, and J. L. Lemaire, J. Chem. Phys. **124**, 094702 (2006).
[21] T. Zubkov, R. S. Smith, T. R. Engstrom, and B. D. Kay, J. Chem. Phys. **127**, 184707 (2007).
[22] W. Rudzinksi and D. H. Everett, *Adsorption of Gases on Heterogeneous Surfaces* (Academic Press, San Diego, 1992).
[23] T. Zubkov, R. S. Smith, T. R. Engstrom, and B. D. Kay, J. Chem. Phys. **127**, 184708 (2007).
[24] R. A. Baragiola, C. L. Atteberry, D. A. Bahr, and M. M. Jakas, Nucl. Instrum. Methods Phys. Res. B **157**, 233 (1999).